Construction, Analysis, Ligation, and Self-Assembly of DNA Triple Crossover Complexes

Thomas H. LaBean,[†] Hao Yan,[‡] Jens Kopatsch,[‡] Furong Liu,[‡] Erik Winfree,[§] John H. Reif,*[,†] and Nadrian C. Seeman*[,‡]

Contribution from the Department of Computer Science, Duke University, Durham, North Carolina 27707, Department of Chemistry, New York University, New York, New York 10003, and Computer Science and Computation and Neural Systems, California Institute of Technology, Pasadena, California 91125

Received September 20, 1999

Abstract: This paper extends the study and prototyping of unusual DNA motifs, unknown in nature, but founded on principles derived from biological structures. Artificially designed DNA complexes show promise as building blocks for the construction of useful nanoscale structures, devices, and computers. The DNA triple crossover (TX) complex described here extends the set of experimentally characterized building blocks. It consists of four oligonucleotides hybridized to form three double-stranded DNA helices lying in a plane and linked by strand exchange at four immobile crossover points. The topology selected for this TX molecule allows for the presence of reporter strands along the molecular diagonal that can be used to relate the inputs and outputs of DNA-based computation. Nucleotide sequence design for the synthetic strands was assisted by the application of algorithms that minimize possible alternative base-pairing structures. Synthetic oligonucleotides were purified, stoichiometric mixtures were annealed by slow cooling, and the resulting DNA structures were analyzed by nondenaturing gel electrophoresis and heat-induced unfolding. Ferguson analysis and hydroxyl radical autofootprinting provide strong evidence for the assembly of the strands to the target TX structure. Ligation of reporter strands has been demonstrated with this motif, as well as the self-assembly of hydrogen-bonded two-dimensional crystals in two different arrangements. Future applications of TX units include the construction of larger structures from multiple TX units, and DNA-based computation. In addition to the presence of reporter strands, potential advantages of TX units over other DNA structures include space for gaps in molecular arrays, larger spatial displacements in nanodevices, and the incorporation of well-structured out-of-plane components in two-dimensional arrays.

Introduction

DNA has been well-known for over 50 years as the genetic material of living systems. Our understanding of the chemical basis for its genetic role[1] has led to the explosive growth of molecular biology since the 1950s and its application in molecular biotechnology since the 1970s. Recently, two new fields have aimed to exploit the chemical properties of DNA: These are DNA nanotechnology[2,3] and DNA-based computation.[4,5] The goals of DNA nanotechnology include the construction of nanoscale objects[6−8] and devices[9] from DNA, as well as the self-assembly of periodic arrays.[2,10−12] DNA nanotechnology takes advantage of the fact that the intermolecular interactions of DNA are diverse, highly specific, and readily programmed through Watson−Crick complementarity. This complementarity can be used to design the spontaneous assembly of single strands into double helices, branched junctions,[2] or more complex motifs.[13] In addition, the Watson−Crick complementary associations of single-stranded overhangs ("sticky ends") can be used in the same way, to direct the specific intermolecular associations of these DNA complexes into more intricate arrangements; examples of such structures range from the linear assembly of DNA molecules that led to the current biotechnology explosion,[14] the assembly of branched molecules into geometrical and topological target figures[6−8] and devices,[9] and the recent assembly of two-dimensional DNA arrays.[10−12] A particularly important feature of sticky-ended association is that the product has a predictable local geometry.[15] These same properties have also led to the adoption of DNA as a popular molecule for molecular computation. One goal of molecular

* Address correspondence to these authors at reif@cs.duke.edu or ned.seeman@nyu.edu.
[†] Duke University.
[‡] New York University.
[§] California Institute of Technology.

(1) Watson, J. D.; Crick, F. H. C. *Nature* **1953**, *171*, 737−738.
(2) Seeman, N. C. *J. Theor. Biol.* **1982**, *99*, 237−247.
(3) Seeman, N. C. *Annu. Rev. Biophys. Biomol. Struct.* **1998**, *27*, 225−248.
(4) Adleman, L. *Science* **1994**, *266*, 1021−1024.
(5) Reif, J. H. In *Unconventional Models of Computation*; Calude, C. S., J. Casti, J., Dinneen, M. J., Eds.; Springer Publishers: 1998; pp 72−93.
(6) Chen, J.; Seeman, N. C. *Nature (London)* **1991**, *350*, 631−633.
(7) Zhang, Y.; Seeman, N. C. *J. Am. Chem. Soc.* **1994**, *116*, 1661−1669.
(8) Mao, C.; Sun, W.; Seeman, N. C. *Nature* **1997**, *386*, 137−138.
(9) Mao, C.; Sun, W.; Shen, Z.; Seeman, N. C. *Nature* **1999**, *397*, 144−146.
(10) Winfree, E.; Liu, F.; Wenzler, L. A.; Seeman, N. C. *Nature* **1998**, *394*, 539−544.
(11) Liu, F.; Sha, R.; Seeman, N. C. *J. Am. Chem. Soc.* **1999**, *121*, 917−922.
(12) Mao, C.; Sun, W.; Seeman, N. C. *J. Am. Chem. Soc.* **1999**, *121*, 5437−5443.
(13) Seeman, N. C. *Angew. Chem., Int. Ed.* **1998**, *37*, 3220−3238.
(14) Cohen, S. N.; Chang, A. C. Y.; Boyer, H. W.; Helling, R. B. *Proc. Nat. Acad. Sci. U.S.A.* **1973**, *70*, 3240−3244.
(15) Qiu, H.; Dewan, J. C.; Seeman, N. C. *J. Mol. Biol.* **1997**, *267*, 881−898.

10.1021/ja993393e CCC: $19.00
Published on Web 00/00/0000 PAGE EST: 12.8

computation is to solve previously intractable problems by utilizing the enormous parallelism that can be derived from the high diversity of molecular species confined to a relatively small volume. It is likely that DNA objects and devices will also contribute to DNA-based computing.

DNA nanotechnology[2,3] and some of the approaches to DNA-based computing[16−18] are dependent on unusual motifs of DNA. The key feature of the most useful motifs is that they contrast with normal DNA in that their helix axes are not strictly linear, but are arranged to flank branch points. The most prominent unusual DNA motif is the immobile DNA branched junction,[2,19] a stable analogue of the Holliday[20] intermediate in genetic recombination. Branched molecules have been constructed that contain three,[21] four,[22] five,[23] or six[23] helices flanking a branch point. Other unusual motifs have included knots,[24] antijunctions and mesojunctions,[25] and double crossover (DX) molecules.[26]

One powerful technique for constructing DNA nanostructures and for performing DNA-based computation is to use the self-assembly of DNA tilings. Wang tiles are theoretical constructs that contain colored edges, and they assemble so that edges with the same colors abut, much like dominoes.[27] It is straightforward to imagine placing four-arm DNA branched junctions at the centers of square tiles, with their helix axes directed normal to the edges. Equating complementary sticky ends with the colored edges reduces the Wang tiles to a concrete self-assembling molecular form, using the medium of DNA.[16] Whereas the assembly of Wang tiles can emulate the operation of a Turing machine,[28] assembling branched junctions in this fashion can lead to meaningful computation; it has been shown that self-assembled arrays of DNA molecules can be used in principle as cellular automata.[16] Thus, experimentally, DNA molecules, referred to here as DNA tiles, can be designed to self-assemble into arrays such as those of Wang tiles through the associations of specific sticky ends. Previous demonstrations of large scale two-dimensional DNA self-assemblies[10−12] can be regarded as experimental verification of the feasibility of such tilings. However, the self-assembly of DNA tilings used for computation has not yet been demonstrated experimentally. The success of the self-assembly approach will depend critically on advances in the design of the individual DNA tiles.

Like the Holliday junction, the DNA double crossover molecule[26] (DX) is an analogue of intermediates in genetic recombination, both meiotic recombination[29] and recombination mediated by double strand breaks.[30,31] The DX molecule consists of two double helical domains joined twice at crossover points; another way to think of the DX molecule is that it is formed from two four-arm branched molecules that have been ligated at adjacent arms. There are five unique motifs to the DX molecule, illustrated in Figure 1a. The three parallel DX motifs, DPE, DPOW, and DPON, are relevant to biological processes, but they are not stable when the separations between their crossovers are two turns or fewer.[26] By contrast, the antiparallel DX molecules, DAE and DAO are stable and well behaved, both in solution, and when analyzed on nondenaturing polyacrylamide gels.[26]

The DAE molecule contains an even number of double helical half-turns between crossover points, whereas the separation in the DAO molecule is an odd number of half-turns. One consequence of this difference is that the DAO molecule consists of four strands of DNA, but the DAE molecule contains an additional cyclic molecule between the crossover points; as a practical point, it is difficult to seal this cyclic strand. Recently, we have analyzed DAE molecules in ligation-closure experiments where the ligation is catalyzed by T4 DNA ligase.[32] It is easiest to analyze these experiments if the product of ligation contains a reporter strand, which is a strand whose fate reflects that of the complex. Figure 1b shows that a ligated oligomer of DAE molecules contains a reporter strand, in contrast to DAO molecules. This is the reason that DAE molecules were analyzed before DAO molecules. The striking result of this analysis is that DAE molecules appear to be quite stiff, in contrast to conventional branched molecules. This finding suggested that DX molecules would be useful for the construction of large DNA arrays: In fact, they have been used recently to construct large arrangements of DNA both in one dimension[33] and in two dimensions;[10,11] although not yet analyzed in the same way, DAO molecules have also proved to be rigid enough to form two-dimensional arrays.[10] Winfree has demonstrated that DX molecules can also be used as cellular automata.[16]

Both DNA nanotechnology and DNA-based computing would benefit from a greater diversity of DNA motifs, particularly those based on branched molecules. One particular motif that would be valuable to both efforts is the triple crossover molecule (TX), illustrated in Figure 1c. There is opportunity for confusion about this name: We use the term “triple crossover” to describe a motif with three adjacent helical domains (parallel or antiparallel) held together by two or more sets of crossover sites between each helical domain; this term is not used to describe a double crossover molecule containing three sites of crossover between two helical domains. The introduction of a third helical domain also introduces the possibility that the three helix axes need not be coplanar, but here we will describe the characterization of a molecule in which the three helix axes are designed to be coplanar as nearly as possible. As shown in Figure 1c, each helical domain is antiparallel to the one adjacent to it; this can be seen because minor grooves abut major grooves in both interhelical regions. There are four crossover points in the molecule; each vertical pair of crossovers is separated by an odd number of half-turns, three between the left two helices and five between the right two helices; thus, if one considers the TX molecule to be composed of two DX molecules that share the central double helix, then both of these DX molecules

(16) Winfree, E. In *DNA Based Computing*; Lipton, E. J., Baum, E. B., Eds.; Am. Math. Soc.: Providence; 1996; pp 199−219.
(17) Reif, J. H. *DNA-Based Computers III*; Rubin, H., Wood, D., Eds.; Providence: Am. Math. Soc. 1998; pp 217−254.
(18) Janoska, N.; Karl, S. A.; Saito, M. *DNA-Based Computers III*; Rubin, H., Wood, D., Eds.; Providence: Am. Math. Soc. 1998; pp 123−136.
(19) Seeman, N. C.; Kallenbach, N. R. *Annu. Rev. Biophys. Biomol. Struct.* **1994**, *23*, 53−86.
(20) Holliday, R. *Genet. Res.* **1964**, *5*, 282−304.
(21) Ma, R.-I.; Kallenbach, N. R.; Sheardy, R. D.; Petrillo, M. L.; Seeman, N. C. *Nucl. Acids Res.* **1986**, *14*, 9745−9753.
(22) Kallenbach, N. R.; Ma, R.-I.; Seeman, N. C. *Nature* **1983**, *305*, 829−831.
(23) Wang, Y.; Mueller, J. E.; Kemper, B.; Seeman, N. C. *Biochemistry* **1991**, *30*, 5667−5774.
(24) Du, S. M.; Stollar, B. D.; Seeman, N. C. *J. Am. Chem. Soc.* **1995**, *117*, 1194−1200.
(25) Du, S. M.; Zhang, S.; Seeman, N. C. *Biochemistry* **1992**, *31*, 10955−10963.
(26) Fu, T.-J.; Seeman, N. C. *Biochemistry* **1993**, *32*, 3211−3220.
(27) Wang, H. *Proc. Symp. Math. Theory of Automata*; Polytechnic Press: New York, 1963; pp 23−26.
(28) Wang, H. *Fundam. Math.* **1975**, *82*, 295−305.
(29) Schwacha, A.; Kleckner, N. *Cell* **1995**, *83*, 783−791.
(30) Thaler, D. S.; Stahl, F. W. *Annu. Rev. Genet.* **1988**, *22*, 169−197.
(31) Sun, H.; Treco, D.; Szostak, J. W. *Cell* **1991**, *64*, 1155−1161.
(32) Li, X.; Yang, X.; Qi, J.; Seeman, N. C. *J. Am. Chem. Soc.* **1996**, *118*, 6131−6140.
(33) Yang, X.; Wenzler, L. A.; Qi, J.; Li, X.; Seeman, N. C. *J. Am. Chem. Soc.* **1998**, *120*, 9779−9786.

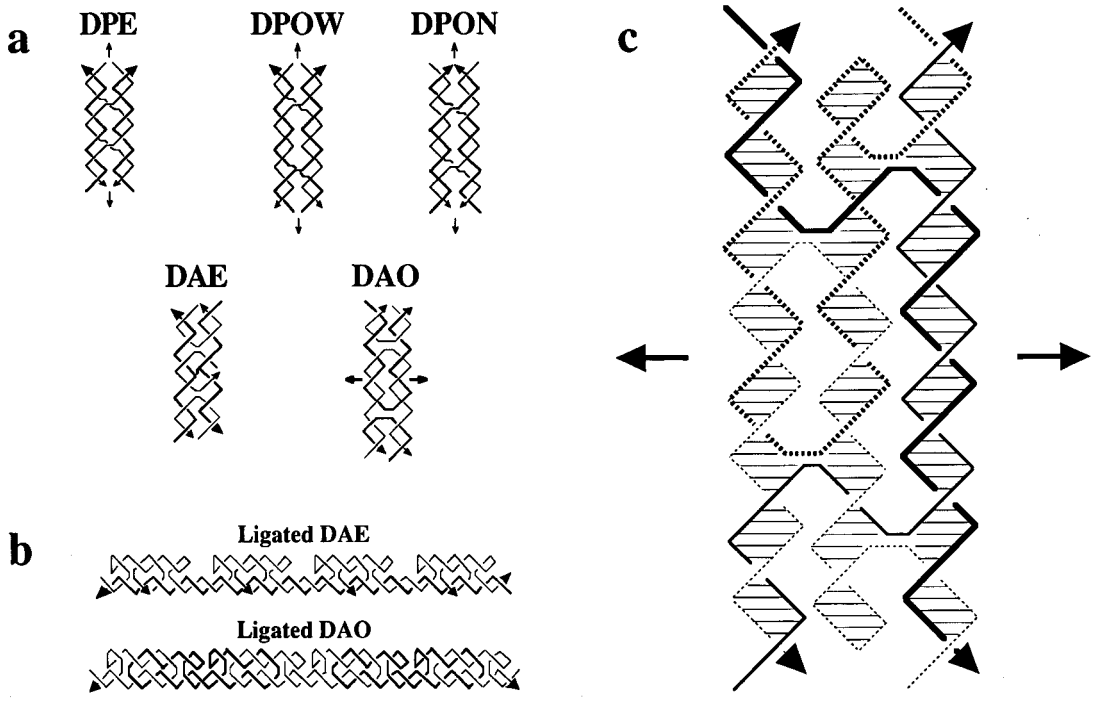

Figure 1. Motifs and ligation of double and triple crossover molecules. (a) Double crossover motifs. The top row contains the three parallel isomers of double crossover (DX) molecules, DPE, DPOW, and DPON; "P" in their name indicates their parallel structure. Arrowheads indicate 3′ ends of strands. Strands drawn with the same thickness are related by the vertical dyad axis indicated in the plane of the paper. DPE contains crossovers separated by an even number (two) of half-turns of DNA, DPOx by an odd number; in DPOW, the extra half-turn is a major groove spacing, in DPON, it is a minor groove spacing. The middle row illustrates two other DX isomers, DAE and DAO. The symmetry axis of DAE is normal to the page (and broken by the nick in the central strand); the symmetry axis of DAO is horizontal within the page; in the case of DAO, strands of opposite thickness are related by symmetry. (b) Ligation products of double crossover molecules. Ligations of the DAE and DAO molecules are shown, where one domain has been capped by hairpins. Ligation of DAE leads to a reporter strand, drawn with a thicker line, but ligation of DAO leads to a polycatenated structure. (c) The TX complex constructed here. The molecule contains three helices, designed to have their axes coplanar. The molecule is composed of four strands, two of which are drawn with solid lines (one thick, one thin), and two drawn with dotted lines; arrows indicate the 3′ ends of strands. The three helical domains are indicated by horizontal stripes that correspond roughly to base pairs; thus, the crossover points are the connections between the domains. The middle helices are capped with hairpin loops. The two arrows horizontal within the plane of the page indicate the dyad axis relating the two pairs of strands to each other: The continuous strands are related to each other by this axis, and the dotted strands are also related to each other by this axis.

are DAO molecules. Other topologies can be designed, e.g., using DAE topologies exclusively, or mixing DAO with DAE, but they have not been explored experimentally.

There are at least three reasons to construct a TX molecule with this topology:

[1] The TX molecules accommodate reporter strands that involve all helical domains. The TX molecule with a double DAO framework can contain a reporter strand that extends diagonally across all the domains; the two strands drawn with solid lines in Figure 1c are reporter strands. This makes the molecule potentially valuable to use for output of data in DNA-based computing: (i) a structure consisting of multiple self-assembled TX molecules is constructed; (ii) the reporter strands of contiguous TX molecules are ligated; (iii) the structure is melted; and (iv) the ligated reporter strands are isolated. These reporter strands provide confirmation of the assembly and allow for determination of the outputs of the computation.

[2] The TX molecules provide space for gaps in molecular arrays. One of the goals of constructing lattices is to produce cavities in the lattice that can accommodate guest macromolecules[2] or molecular electronic species.[34] This can be achieved with DX molecules, as shown at the top of Figure 2a. However, an array of TX molecules is a natural and convenient way to generate a one-helix gap at a high density with only a single species in the array, as shown in Figure 2a.

[3] The TX molecules allow for large displacements in nanomechanical devices. The maximum displacement of an atom in a recently described DNA nanomechanical device[9] predicated on two DX molecules is about 60 Å. However, with TX components, a displacement of 100 Å could be achieved, as shown in Figure 2b.

Here, we describe the construction of a TX molecule and characterize its structure by nondenaturing gel electrophoresis, Ferguson analysis, hydroxyl radical autofootprinting, and thermal transition analysis. We find that this molecule is well-behaved, and that it appears be at least as tractable as the DX molecule for applications that involve both DNA nanotechnology and DNA-based computing. We demonstrate that it is possible to ligate these molecules to produce reporter strands that could be used as the output strands of a DNA computation. In addition, we demonstrate that it is possible to produce two-dimensional arrays from these molecules and to visualize them by means of atomic force microscopy.

Materials and Methods

Synthesis and Purification of DNA. Custom oligonucleotides were purchased from Integrated DNA Technology (www.idtdna.com) or were synthesized on an Applied Biosystems 380B synthesizer using routine phosphoramidite chemistry.[35] DNA strands have been purified by electrophoresis; bands are cut out of 12−20% denaturing gels and eluted in a solution containing 500 mM ammonium acetate, 10 mM magnesium acetate, and 1 mM EDTA.

(34) Robinson, B. H.; Seeman, N. C. *Prot. Eng.* **1987**, *1*, 295−300.
(35) Caruthers, M. H. *Science* **1985** *230*, 281−285.

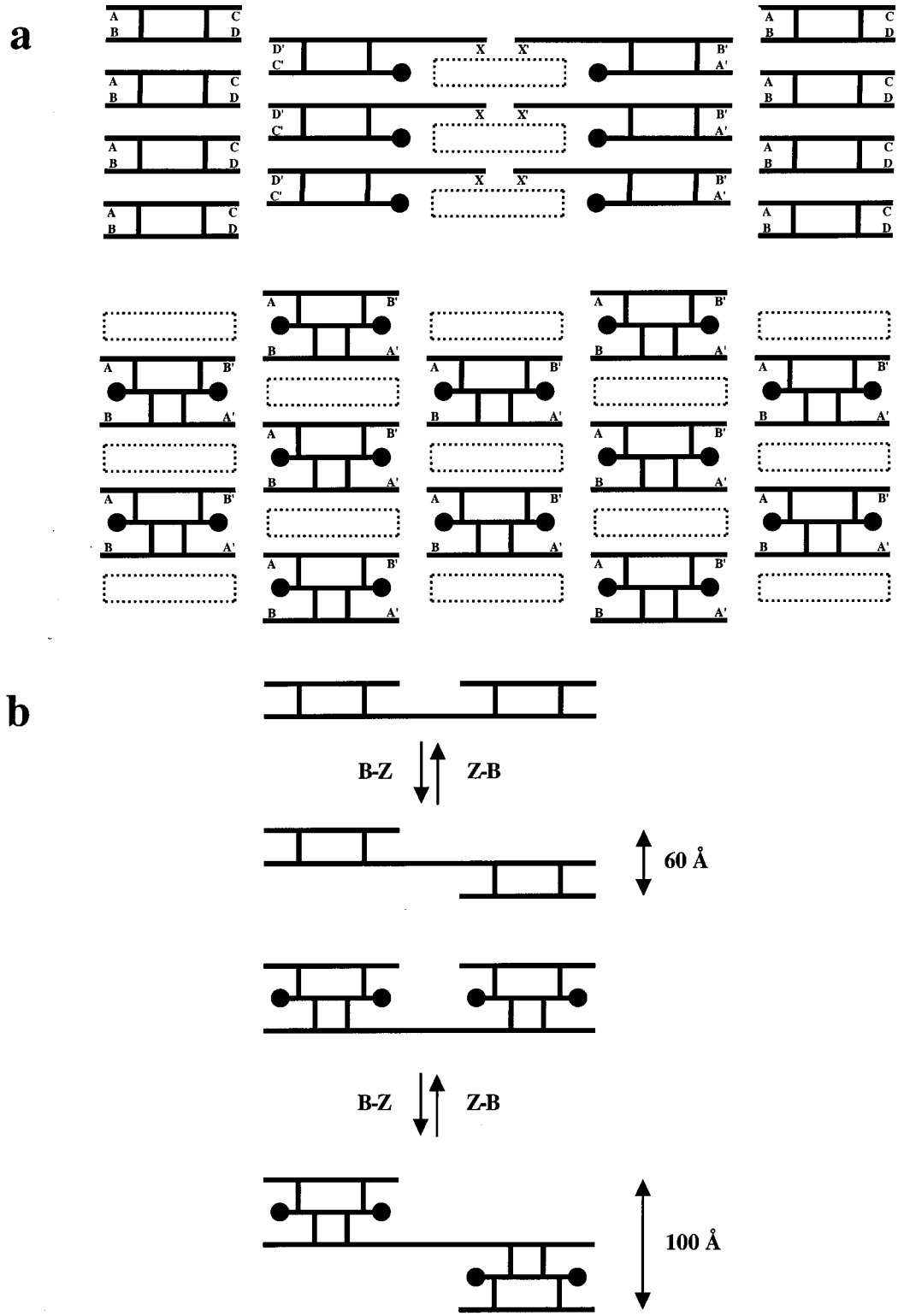

Figure 2. Possible uses for TX molecules. (a) The creation of cavities in DX and TX lattices. The upper diagram illustrates that three DX molecules can be used to create a continuous two-dimensional lattice containing a cavity whose width is a single DNA double helix. The molecules on the far left and far right are the same DX molecule, and they represent a lattice repeat in the horizontal direction. The two molecules in the middle are two DX molecules containing an extended helical domain and a helical domain capped by a hairpin loop, represented by a filled circle. A dotted rectangle between these two molecules represents the cavity. The letters represent complementary sticky ends designed to stabilize the lattice. The vertical row of DX molecules with sticky ends A, B, C, and D stabilizes the other DX molecules in the vertical direction. The lower diagram illustrates that a single TX molecule could produce the same cavity easily. (b) Nanomechanical devices predicated on the B−Z transition constructed from DX and TX components. The upper drawing illustrates a recently reported nanomechanical device constructed from DX molecules. The maximum excursion of an atom from the top to the bottom of the displaced helix is about 60 Å, the diameter of three DNA double helices. The bottom drawing illustrates the same device constructed from TX molecules. In this case, the maximum displacement is about 100 Å, the diameter of five DNA double helices.

Formation of Hydrogen-Bonded Complexes. Complexes are formed by mixing a stoichiometric quantity of each strand, as estimated by OD_{260}. This mixture is then heated to 90 °C for 5 min and cooled to the desired temperature by the following protocol: 20 min at 65 °C,

Table 1. Sequences Used in These Studies

I. The Molecule Characterized Extensively by Solution Techniques

strand 1:
5′-TTGGCTATCG.AGTGGACACC.GAAGACCTAA.CCGCTTTGCG.TTCCTGCTCT.AC-3′ = 52
strand 2:
5′-GTTCAGCCTT.AGTGGAGTGG.AACGCAAAGC.GGTTAGGTCT.TCGGACGCTC.GT-3′ = 52
strand 3:
5′-ACGAGCGTGG.TAGTTTTCTA.CCTGTCCTGC.GAATGAGATG.CCACCACAGT.CACGGATGGA.CTCGATAGCC.AA-3′ = 72
strand 4:
5′-GTAGAGCACC.AGATTTTTCT.GGACTCCTGG.CATCTCATTC.GCACCATCCG.TGACTGTGGA.CTAAGGCTGA.AC-3′ = 72

II. The Molecules of the AB* Array:

II.1. molecule A

strand 1:
5′-TCGGCTATCG.AGTGGACACC.GAAGACCTAA.CCGCTTTGCG.TTCCTGCTCT.AC-3′ = 52
strand 2:
5′-AGTTAGTGGA.GTGGAACGCA.AAGCGGTTAG.GTCTTCGGAC.GCTCGTGCAA.CG-3′ = 52
strand 3:
5′-ACGAGCGTGG.TAGTTTTCTA.CCTGTCCTGC.GAATGAGATG.CCACCACAGT.CACGGATGGA.CTCGAT-3′ = 66
strand 4:
5′-TGCTCGGTAG.AGCACCAGAT.TTTTCTGGAC.TCCTGGCATC.TCATTCGCAC.CATCCGTGAC.TGTGGACTAA.CTCCGCTT-3′ = 78

II.2. molecule B*

strand 1:
5′-CGAGCAATGA.AGTGGTCACC.GTTATAGCCT.GGTAGTGAGC.TTCCTGCTGT.AT-3′ = 52
strand 2:
5′-ACACAGTGGA.GTGGAAGCTC.ACTACCAGGC.TATAACGGAC.GATGATAAGC.GG-3′ = 52
strand 3:
5′-AGCCGAATAC.AGCACCATCT.TTTGATGGAC.TCCTGAATCG.ACGTAACTTT.TGTTACGTCT.TTCTACTCGC.ACCTTCGCTG.
AGTTTGGACT.GTGTCGTTGC-3′ = 100
strand 4:
5′-ATCATCGTGG.TTCTTTTGAA.CCTGACCTGC.GAGGTATGTG.ATTTTTCACA.TACTTTAGAG.ATTCACCAAA.
CTCAGCGAAG.GACTTCAT-3′ = 88

III. The Molecules of the ABC′D Array:

III.1. molecule A

strand 1:
5′-GATTGCCGAC.CGCAAGCGTG.GAGTGGCATC.GTAAGTCACA.TTCAATACGG.ACAAGTAACG.AC-3′ = 62
strand 2:
5′-GTCGTGCCTA.ACAGTTGGAC.TCCTGATGTC.TACGCCAGTG.GTCATCTGGT.ATCGGACGCT.TGCGGTCG-3′ = 68
strand 3:
5′-GCTTCGCTGA.CAGCCTGAGG.ACTGGCGTAG.ACATCACCG.ATACCAGATGA.CCTGCGAGTA.TGCT-3′ = 64
strand 4:
5′-CAGACGAGCA.TACTCGCACC.TCACCGTATT.GAATGTGACT.TACGATGCCT.GTAGCGGATA.GC-3′ = 62
strand 5:
5′-TCAACGGCTA.TCCGCTACAC.CAACTGTTAG.G-3′ = 31
strand 6:
5′-AGCAGTGTCG.TTACTTGTGG.CTGTCAG-3′ = 27

III.2. molecule B

strand 1:
5′-ACTGCTCGTT.CATGCGACAC.CGCACCAAGT.GATAGACACT.GTATGACGCC.TGAACTGATG.AGC-3′ = 63
strand 2:
5′-GTCAGCCGAT.ACGATGCCTG.CGGACATCCA.GTCACGGCAC.CTATGCTGTG.CTACCTGTCG.CATGAACG-3′ = 68
strand 3:
5′-GACCAGCGTA.GATGGACTCC.TGCCGTGACT.GGATGTGGTA.GCACAGCATA.GGACTAAGCA.ACTAC-3′ = 65
strand 4:
5′-CGTTGAGTAG.TTGCTTAGTG.GAGTGGCGTC.ATACAGTGTC.TATCACTTGG.ACGACGGTCA.AGC-3′ = 63
strand 5:
5′-CGTCTGGCTT.GACCGTCGTG.GCATCGTATC.G-3′ = 31
strand 6:
5′-GCAATCGCTC.ATCAGTTCAC.CATCTACG-3′ = 28

III.3. molecule C′

strand 1:
5′-GCAGTTAGCG.TCACCAGTGG.CGTGATACAT.CTGTTGACCT.ATCCTGCTAC.GCATTCG-3′ = 57
strand 2:
5′-CGAAGCGACA.CTCGGACTGG.ACTACCAGCA.ATCGCACCGT.ATGTCTGATG.CCTGACGCTA.ACTGC-3′ = 65
strand 3:
5′-CACGACCGCT.CACTTGGACT.CCTGCGATTG.CTGGTAGTGG.CATCAGACAT.ACGGACAGCC.GATGGTC-3′ = 67
strand 4:
5′-GACCATCGGC.TGTGGAGTGG.ATAGGTCAAC.AGATGTATCA.CGCCTGAACG.TGCCGTC-3′ = 57

Table 1 (Continued)

III.3. molecule C′
strand 5: 5′-GACGGCACGT.TCACCGAGTG.TC-3′ = 22 strand 6: 5′-CGAATGCGTA.GCACCAAGTG.AGCG-3′ = 24
III.4. molecule D
strand 1: 5′-CTGGTCGCAC.TACGGCAGTA.TGGCTATCGT.GATGTAACCG.CTTGTCACTG.GC-3′ = 52 strand 2: 5′-GCTGACGCCA.GTGACAAGCG.GTTACATCAC.GATAGCCATA.CTGCCGTAGT.GC-3′ = 52

20 min at 45 °C, 30 min at 37 °C, 30 min at room temperature, and (if desired) 30 min at 4 °C. Exact stoichiometry is determined, if necessary, by titrating pairs of strands designed to hydrogen bond together, and visualizing them by nondenaturing gel electrophoresis; absence of monomer is taken to indicate the endpoint.

Nondenaturing Polyacrylamide Gel Electrophoresis. Gels contain 8% acrylamide (19:1, acrylamide:bisacrylamide) and a buffer consisting of 40 mM Tris-HCl (pH 8.0), 20 mM boric acid, 2 mM EDTA, and 12.5 mM magnesium acetate (TAEMg). The DNA is dissolved in 10 μL of NEBuffer 2 (New England Biolabs) or in water. Tracking dye (1 μL) containing TAEMg, 50% glycerol, and 0.2% each of Bromophenol Blue and Xylene Cyanol FF is added to the sample buffer. Gels are run on a Hoefer SE-600 electrophoresis unit at 4 V/cm at room temperature and exposed to X-ray film for up to 15 h or stained with Stains-all (0.01% Stains-All from Sigma, 45% formamide) and then photographed.

Phosphorylation. Ten picomoles of an individual strand of DNA are dissolved in 25 μL of a solution containing 66 mM Tris·HCl, pH 7.6, 6.6 mM $MgCl_2$, 10 mM dithiothreitol (DTT), and mixed with 6 μL of 2.2 μM γ-^{32}P-ATP (10 mCi/mL) and 6 units of polynucleotide kinase (US Biochemical) for 90 min at 37 °C. The reaction is stopped by heating the solution to 90 °C for 10 min, followed by gel purification.

Ligation. Ligations are performed in the kination buffer, which has been brought to 1 mM in ATP. One unit of T4 polynucleotide ligase (Amersham) is added, and the reaction is allowed to proceed at 16 °C for 7 h. The reaction is stopped by phenol/chloroform extraction. Samples are then ethanol precipitated.

Exonuclease Treatment of the Ligated Array. The sample was heated at 90 °C for 10 min and cooled rapidly on ice to destroy the array and to avoid reannealing. Ten units of exonuclease I and 200 units of exonuclease III (Amersham) were used to remove all linear ligation products by incubation at 37 °C for 1 h.

Hydroxyl Radical Autofootprinting Analysis. Individual strands are radioactively labeled and are additionally gel purified from a 10−20% denaturing polyacrylamide gel. Each of the labeled strands [approximately 1 pmol in 50 mM Tris·HCl (pH 7.5) containing 10 mM $MgCl_2$] is annealed to a 10-fold excess of the unlabeled complementary strands, or it is annealed to a 10-fold excess of a mixture of the other strands forming the complex, or it is left untreated as a control, or it is treated with sequencing reagents[36] for a sizing ladder. The samples are annealed by heating to 90 °C for 3 min and then cooled slowly to 4 °C. Hydroxyl radical cleavage[37,38] of the double-strand and TX-complex samples for all strands takes place at 4 °C for 2 min. The reaction is stopped by the addition of thiourea. The sample is dried, dissolved in a formamide/dye mixture, and loaded directly onto a 10−20% polyacrylamide/8.3 M urea sequencing gel. Autoradiograms are analyzed on a BioRad GS-525 Molecular Imager.

Thermal Denaturation Profiles. DNA strands were dissolved to 1 μM concentration in 2 mL of a solution containing 40 mM sodium cacodylate, and 10 mM magnesium acetate, pH 7.5, and annealed as described above. The samples were transferred to quartz cuvettes, and the cacodylate buffer was used as a blank. Thermal denaturation was monitored at 260 nm on a Spectronic Genesys 5 Spectrophotometer, using a Neslab RTE-111 circulating bath; temperature was incremented at 0.1 °C /min. Slow annealing of samples was found to be particularly important to avoid artifacts.

Array Assembly. All strands for a given TX array are mixed in 20 mM Tris (pH 7.6), 10 mM $MgCl_2$. The final concentration of DNA is 0.4 μM, and the final volume is 50 μL. The tube containing the DNA solution is put in about 2 L boiled water and placed in a Styrofoam box for at least 40 h to facilitate hybridization.

AFM Imaging. A 3−5 μL aliquot of a solution containing arrays is deposited on a freshly cleaved mica surface for 1.5 min. It is then washed with double distilled water and dried with compressed air. Samples were imaged under 2-propanol in a fluid cell on a Nanoscope II and commercial 100 or 200 μm oxide-sharpened silicon-nitride oriented twin tips (Digital Instruments).

Results

Design of the Complexes. The design of the TX complex analyzed here in detail was based on principles and empirical knowledge gained during the construction and analysis of the simpler DX[26] tiles. For example, lengths of helical runs between crossover points must be in multiples of double helical half-turns to avoid imposing torsional stress on the system. The subsequence used for all hairpins was dT_4. Each crossover point is flanked by two nucleotides of the J1 junction,[39] to produce stable immobile junctions with a well-defined preferred crossover isomer.[38,40]

Subsequences for the complementary regions were chosen by a stochastic hill-climbing algorithm which searched for a set of sequence words that would maximize the selectivity of desired base-pairing and minimize the chance of undesired complementarity. Resulting sequences were checked using SEQUIN.[41] Further TX molecules used for array formation and ligation were designed using SEQUIN. The sequences of all molecules are shown in Table 1.

Complex Assembly. Formation of specific molecular weight complexes by annealing stoichiometric mixtures of all four and various subsets of the four oligonucleotides is shown in the top panel of Figure 3. Each lane (with the exception of the far right lane, discussed below) shows only a single band, demonstrating specific base-pairing without significant unexpected associations. The lane containing only strand 1 (far right) shows dimer formation which is not unusual, because DNA is often seen to base-pair with poorly complementary strands in the absence of a properly matched partner (e.g., ref 32). Strand 1 dimer formation is eliminated by the addition of strands complement-

(36) Maxam, A. M.; Gilbert, W. *Proc. Acad. Sci. U.S.A.* **1977**, *74*, 560−564.
(37) Tullius, T. D.; Dombroski, B. *Science* **1985**, *230*, 679−681.
(38) Churchill, M. E. A.; Tullius, T. D.; Kallenbach, N. R.; Seeman, N. C. *Proc. Acad. Sci. U.S.A.* **1988**, *85*, 4653−4656.
(39) Seeman, N. C.; Kallenbach, N. R. *Biophys. J.* **1983** *44*, 201−209.
(40) Miick, S. M.; Fee, R. S.; Millar, D. P.; Chazin, W. J. *Proc. Nat. Acad. Sci. U.S.A.* **1997**, *94*, 9080−9084.
(41) Seeman, N. C. *J. Biomol. Struct. Dyn.* **1990**, *8*, 573−581.

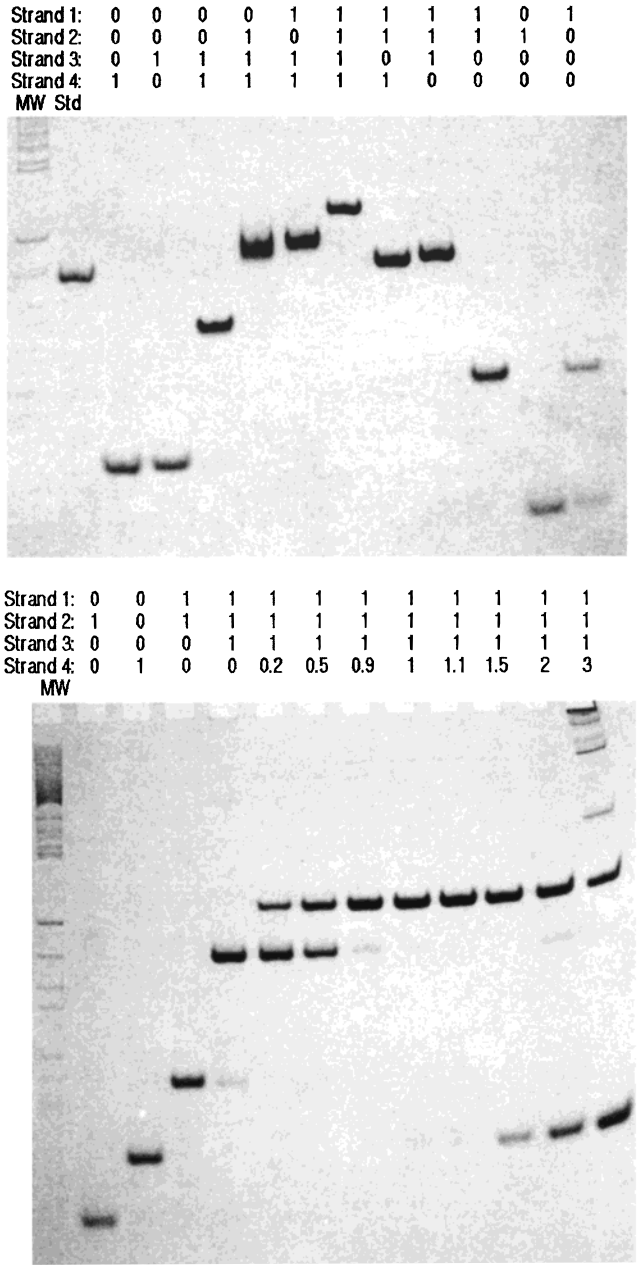

Figure 3. Nondenaturing gels of the TX complex. The top panel shows an 8% stained polyacrylamide gel indicating association complexes between various equimolar combinations of TX component strands. Equimolar mixtures at 3 nM concentration per included strand were annealed and electrophoresed at room temperature. Strands included in the annealing are indicated with a "1" above the lane. Formation of dimer, trimer, and tetramer are shown in the expected lanes. In the bottom panel, the trimeric complex of strands 1, 2, and 3 is titrated with varying amounts of strand 4. The stoichiometric mixture is shown in the lane labeled 1:1:1:1, and strand ratios in other lanes are as indicated. Each strand is present at 3 nM concentration in the equimolar mixture.

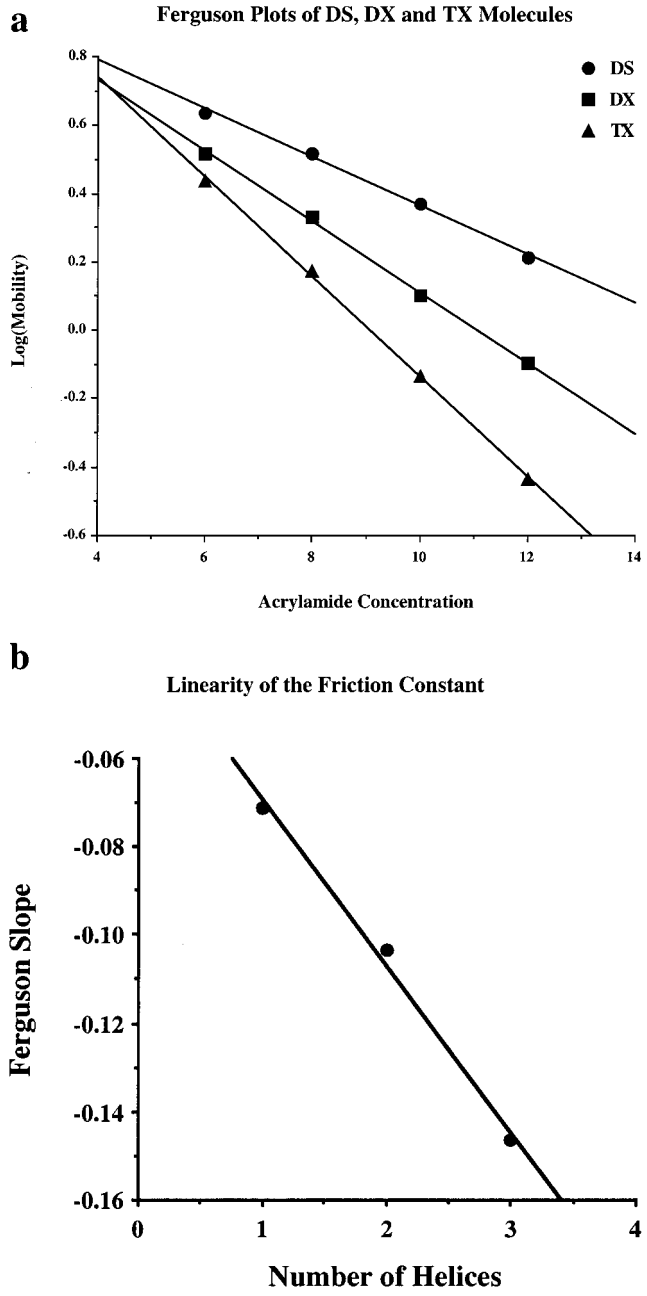

Figure 4. Ferguson analysis. (a) Ferguson plots. Log(mobility) as a function of polyacrylamide concentration is shown for double-stranded DNA (DS, circles), for a double crossover complex (DX, squares) and a triple crossover (TX, triangles). The overall length of each complex is 42 base pairs. The graph shows the log of absolute mobility in cm/h for each of the structures. (b) Analysis of the Ferguson slopes. The increase in relative friction constant with increasing numbers of helical domains in the complex is roughly linear.

ing strand 1; no more slowly moving bands are observed in the other lanes as would be expected if two copies of strand 1 participated in the higher order complexes.

More detailed examination of the stoichiometry of complex formation is shown in the bottom panel of Figure 3. The gel shows titration of a 1:1:1 mixture of stands 1, 2, and 3 with increasing amounts of strand 4. The lane containing 1:1:1:1 stoichiometry (as estimated by OD_{260}) shows a faint amount of three strand complex, indicating slightly less strand 4 than expected. The 1:1:1:1.1 lane appears to give the cleanest tetramer (target) band, while additional strand 4 (1:1:1:1.5) begins build-up of a monomer band. Annealing with 3-fold excess strand 4 (1:1:1:3) generates a large diversity of high molecular weight complexes. The data from these analyses provide initial evidence for formation of TX structure with the target stoichiometry of the designed complex.

Ferguson Analysis. The slope of the Ferguson plot of log(mobility) as a function of polyacrylamide concentration yields information about the surface of a molecule, because the slope of the plot is proportional to its friction constant.[42] Previously, we have examined various unusual DNA motifs using Ferguson

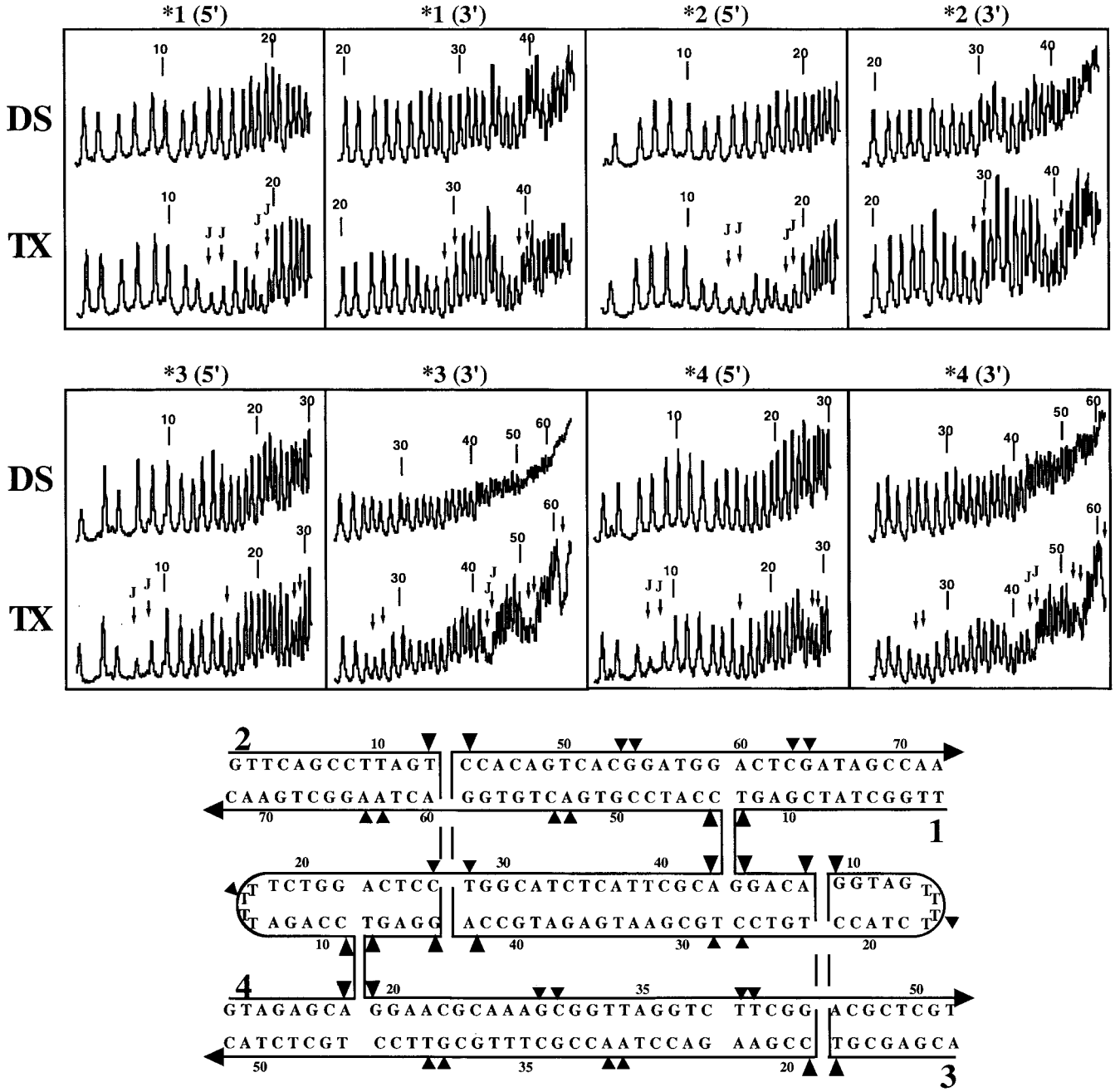

Figure 5. Hydroxyl radical autofootprinting. The top portion of the figure contains densitometer scans of autoradiograms for each strand of the TX molecule. The data for each strand is shown twice, once for its 5′ end, and once for its 3′ end, as indicated above the appropriate panel. Susceptibility to hydroxyl radical attack is compared for each strand when incorporated into the TX molecule (TX) and when paired with its traditional Watson−Crick complement (DS). Nucleotide numbers are indicated above every tenth nucleotide. The two nucleotides flanking expected crossover positions are indicated by two "**J**"s. Note the correlation between the "**J**"s and protection in all cases. Additional protection is seen at further locations, indicating occlusion a turn away from the crossover points on the crossover strands, and about 4 nucleotides 3′ to the crossovers on the helical strands, as noted previously.[38] The data are summarized on a molecular drawing below the scans. Sites of protection are indicated by triangles pointing toward the protected nucleotide; the extent of protection is indicated qualitatively by the sizes of the triangles.

analysis.[22,25,26] Figure 4a shows the results of this analysis for the TX complex, a double crossover (DX) and linear duplex DNA (DS) with equal overall lengths (42 base pairs). The slopes for DS, DX, and TX were −0.0711, −0.1036, and −0.1464, respectively, and intercepts were 1.074, 1.146, and 1.328, respectively. The overall trends of the data are as expected in the series DS, DX, TX. As illustrated in Figure 4b. the increase in relative friction constant is roughly linear in the number of helices, suggesting that the same amount of surface area is added in the step from DX to TX as in the step from DS to DX.

Hydroxyl Radical Autofootprinting Analysis. Quantitative analysis of the cleavage of DNA by reaction with hydroxyl radicals provides an indication of the relative exposure of individual residues to this reagent.[43] The cleavage of a radioactively labeled strand in the TX complex is compared to cleavage in duplex DNA; decreased susceptibility suggests that hydroxyl radical access has been limited by steric factors at

(42) Rodbard, D.; Chrambach, A. *Anal. Biochem.* **1971**, *40*, 95−134.

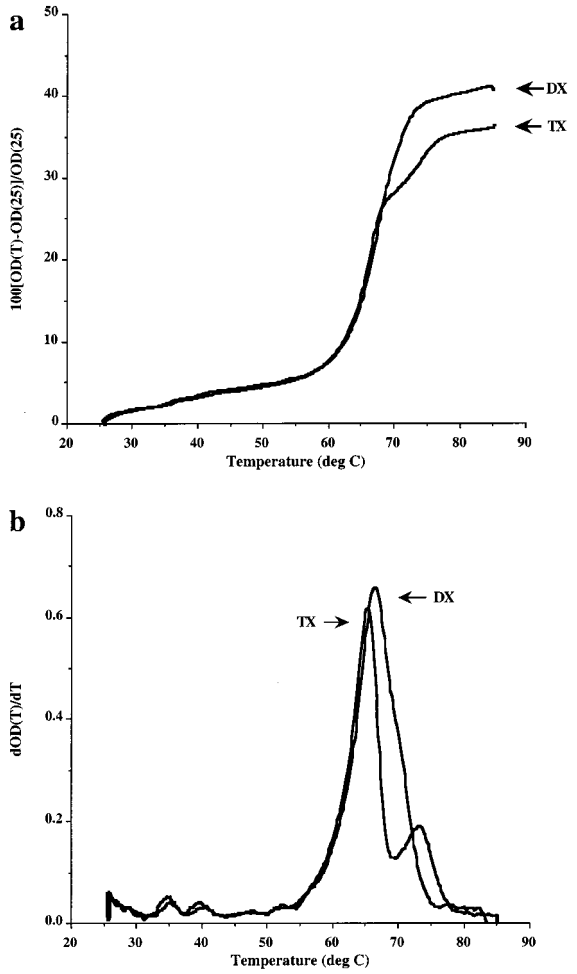

Figure 6. Thermal transition profiles. (a) The relative change in optical density at 260 nm as a function of temperature. The melting behavior of a double crossover (DX) is compared with that of the triple crossover molecule (TX). Although the melting of the DX molecule is uniphasic, the melting of the TX molecule is biphasic. (b) The differential melting behavior of the two species. The TX molecule does not begin to melt before the DX molecule, but its second melting domain melts at a higher temperature.

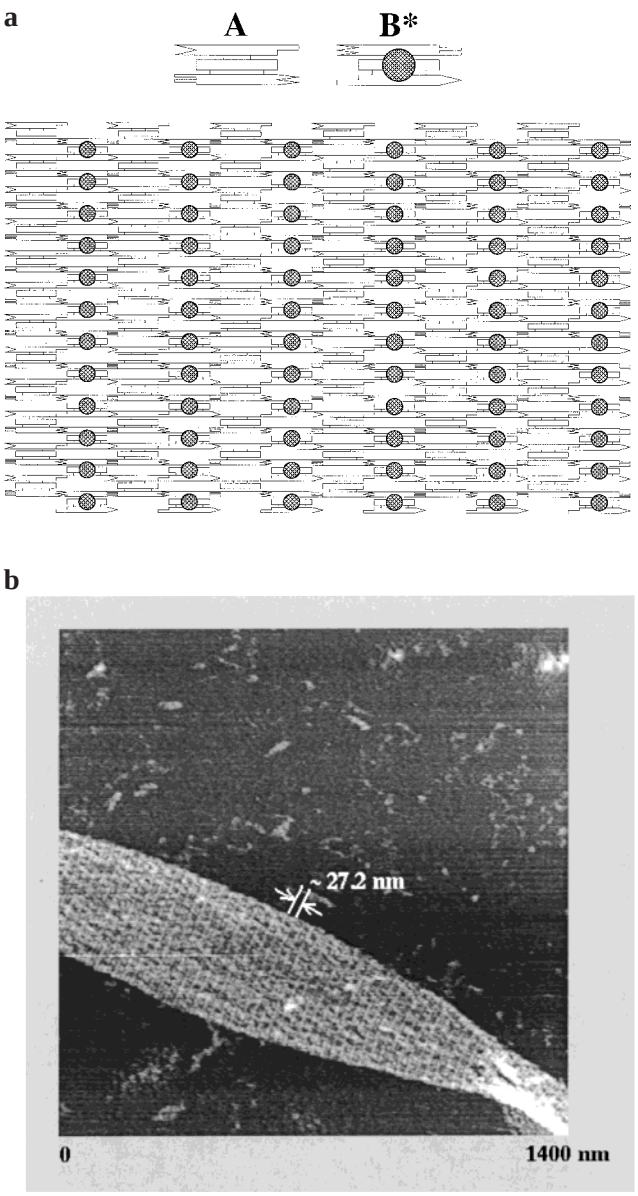

Figure 7. A two-dimensional TX array marked by bulged junctions. (a) Schematic diagram of the array. The two components of the array are shown schematically at the top of the drawing. For clarity, the tiles are foreshortened by roughly a factor of 2. The two tiles are labeled, and each is shaded differently. The sticky ends are shown as complementary geometric shapes. The lack of sticky ends on the central domains is indicated by the short square-ended rectangle in each molecule. **A** is a TX molecule, and **B*** is a TX+2J molecule. Its protruding hairpins are represented by a crosshatched circle. Beneath the components, the array is drawn with the same components reduced in size. The topographic features of the TX+2J molecule appear as stripes (vertical rows of crosshatched circles) in the AFM, whose resolution is sufficient to resolve stripes, but insufficient to resolve individual hairpins packed together with 6 nm spacings. (b) An AFM image of the array drawn in (a). The width of the entire field is 1400 nm. The individual stripes are separated by 27.2 nm, roughly the expected distance of 28.6 nm.

sites where it is observed. In previous studies, protection (decreased susceptibility) has been noted at crossover points and at sites where the surfaces of adjacent helices occlude one another from exposure to hydroxyl radicals.[23,25,26,32,38]

The results of these experiments are shown in Figure 5. Each panel contains a densitometer trace from a lane in the autoradiogram. Owing to the lengths of the strands, the data for the 5′ and 3′ parts each strand are gathered from separate lanes. Information concerning protection and susceptibility is garnered by comparison of band densities from linear duplex (DS) with those from triple-crossover (TX) complex. Nucleotide positions designed to participate in crossover junctions (J) are marked.

Protection from cleavage in the TX complex relative to that in DS is observed at all of the crossover sites, positions 13−14 and 18−19 on both strands 1 and 2, and positions 8−9 and 43−44 on strands 3 and 4. In addition, decreased susceptibility to cleavage is noted at several positions which are predicted to be buried or occluded in the modeled structure; these include positions 28 and 38 on strands 1 and 2, and positions 16, 26−27, and 52−53 on strands 3 and 4. The cleavage footprinting pattern is as expected for DNA participating in the TX complex as designed and modeled. The protection pattern seen is consistent with the structure drawn in Figure 1c.

Thermal Transition Profiles. Melting curves of DNA complexes provide a measure of stability and cooperativity of internal interactions indicated, respectively, by the temperature at the transition midpoint and the width or range of the transition. Figure 6a illustrates the thermal transition profile in

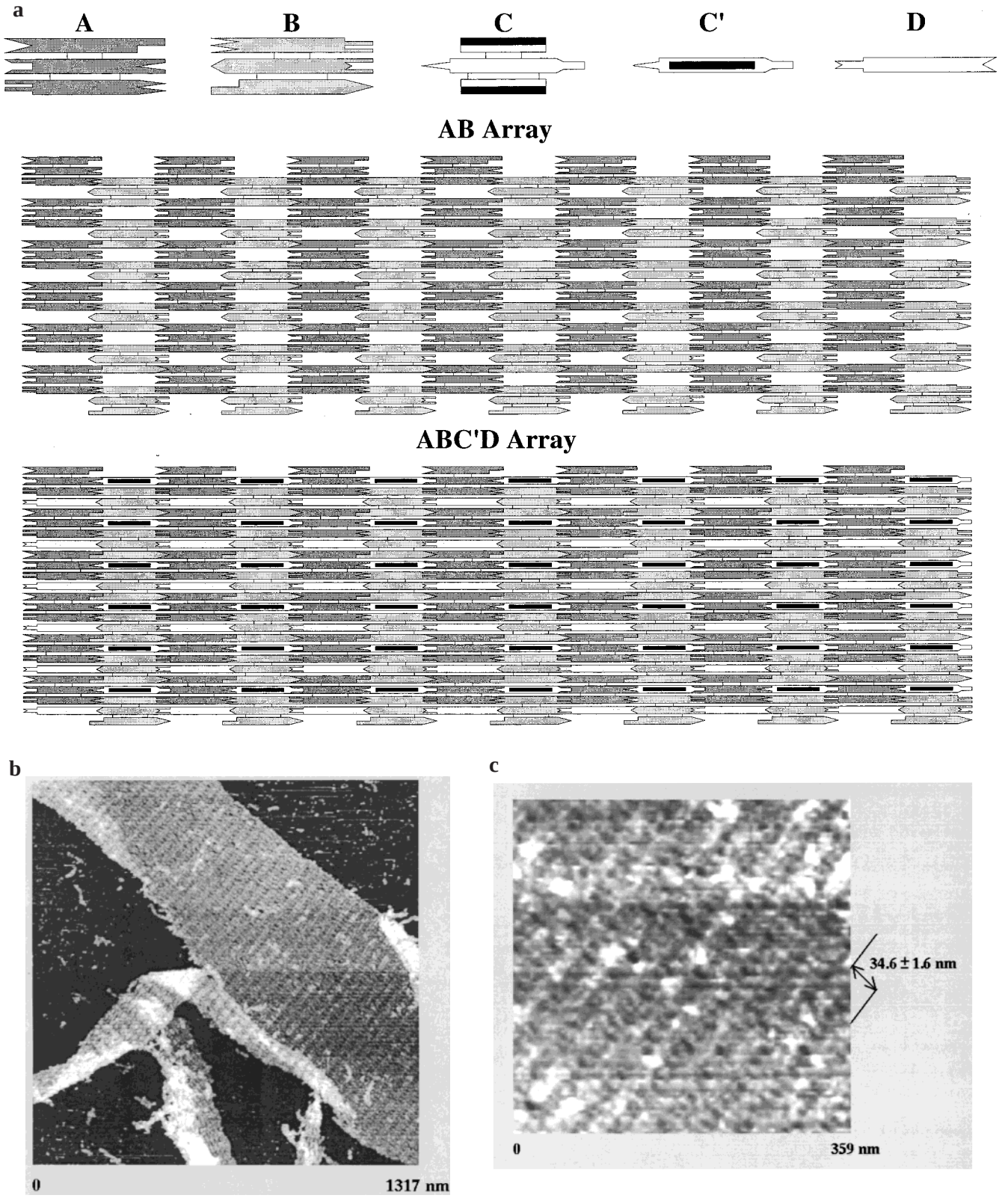

Figure 8. A two-dimensional array composed of two TX molecules, a rotated TX molecule, and a double helical molecule. (a) A schematic drawing of the array. The same conventions apply as in Figure 7. The components of the array are shown at the top of the drawing. **A** and **B** are TX molecules containing sticky ends on all three of their domains. The geometrically represented sticky ends are designed to be complementary so as to produce the **AB** array shown in the drawing. **C** is a third TX molecule, containing only a single pair of sticky ends in its central domain. When its sticky ends pair with those of **A** and **B**, it is rotated about 103° relative to their plane. This rotated molecule is represented as **C′** at the top of the figure. **D** is a conventional double stranded molecule, designed to fill the gaps left in the array. The **ABC′D** array is shown below the **AB** array. Note that the presence of the **C′** units results in raised stripes that will be visible in the AFM. (b) An AFM image of the array. The stripes of the array caused by the presence of the **C′** TX molecule are visible. The nearly rectangular nature of the array is visible. (c) A zoom of (b). The direction of the stripes is parallel to the lines outside the image; separation of the stripes (as deduced from Fourier techniques) is 34.3 ± 1.5 nm, in good agreement with the predicted value of 35.7 nm.

comparison with a DX molecule of the same length and similar base composition (55% GC for the TX molecule, vs 57% for the DX molecule). Figure 6b shows these same data in differential form. The key difference between the two profiles is that the DX molecule melts cooperatively, as a single transition, with T_{max} = 66.4 °C, whereas the TX molecule displays two transitions. The first of these, and by far the most prominent, has T_{max} = 65.2 °C, and the second is somewhat higher, T_{max} = 73.0 °C. A possible origin of this second transition is the presence of hairpin loops on the ends of the central helix, thereby stabilizing substantially the base pairs that flank them.

Self-Assembly of TX Molecules. Both nanotechnological and computational applications of TX molecules are dependent in part on the ability to assemble and visualize them in two-dimensional arrays. We have constructed and visualized two different types of arrays. In one case, we apply a modification of an approach used previously,[10] where we have used two different TX tiles, an **A** tile and a **B*** tile. The **B*** tile is a TX+2J molecule, analogous to the DX+2J[10,11] motif, in that it contains an extra pair of hairpins (on its central helical domain), directed out of the plane of the molecule; this feature produces a periodic topographic pattern in the array, which can be visualized by atomic force microscopy (AFM). A schematic of this arrangement is shown in Figure 7a, and an AFM image of the array is shown in Figure 7b. Each tile contains three helices, each about 20 Å wide, and the repeat distance is four helical turns, corresponding to 42 nucleotides (about 143 Å); hence, their dimensions are approximately 14.3 × 6 nm, so the stripes should be spaced by about 28.6 nm; which is close to that seen in Figure 7b.

In addition to this method of marking distances in the array, we have used a different approach. We have used a set of three TX molecules, **A**, **B**, and **C**. **A** and **B** are conventional TX molecules, in that they contain no extra hairpins. However, their central domain is no longer capped with hairpin loops, but with sticky ends. **C** is also a conventional TX molecule, but its outer domains are capped with hairpin loops, and its central domain contains sticky ends complementary to those of **A** and **B**. Of course, it is not possible to fit **C** into one of the slots between **A** and **B** in the same orientation as **A** and **B**. However, by rephasing it three nucleotide pairs (equivalent to rotating it by roughly 103°), the axes of the two outer helices are placed above and below the plane of **A** and **B**, and the molecule fits nicely. In this orientation its capped helices act as topographic labels; these labels are different from the bulged junctions in DX+2J and TX+2J molecules, but nevertheless, they protrude from the plane of the array. A schematic of this arrangement is shown in Figure 8a, where the rotated **C** molecule is labeled as **C′**. **C′** only fills every other gap in the array, so a duplex molecule, **D**, is used to fill the other gaps. An AFM image can be seen in Figure 8b, and a zoom is shown in Figure 8c. The spacing in this array is 34.3 ± 1.5 nm, in good agreement with the spacing of 35.7 nm expected for 10 helical turns (105 nucleotide pairs).

Ligation of TX Molecules. The use of TX molecules in molecular computation entails the ligation of the diagonal strands, so that they may be used as reporter strands. We have tested the ligatability of these strands when the molecules are arranged in the two-dimensional array. We have used the TX array of Figure 7 for this purpose. Following assembly of the array, the molecules have been ligated together. Figure 9 contains a denaturing gel that shows the results of this ligation. Each of the four strands in each of the two molecules has been labeled separately in this gel, so that eight different ligations are shown. Alternating lanes illustrate the results of loading the products onto the gel directly. These lanes are interspersed by lanes that show the results of treating these products with exonuclease. In no case do any products remain, indicating that no cyclic products have been formed. Thus, linear reporter strands as long as 20 units can be prepared from this system.

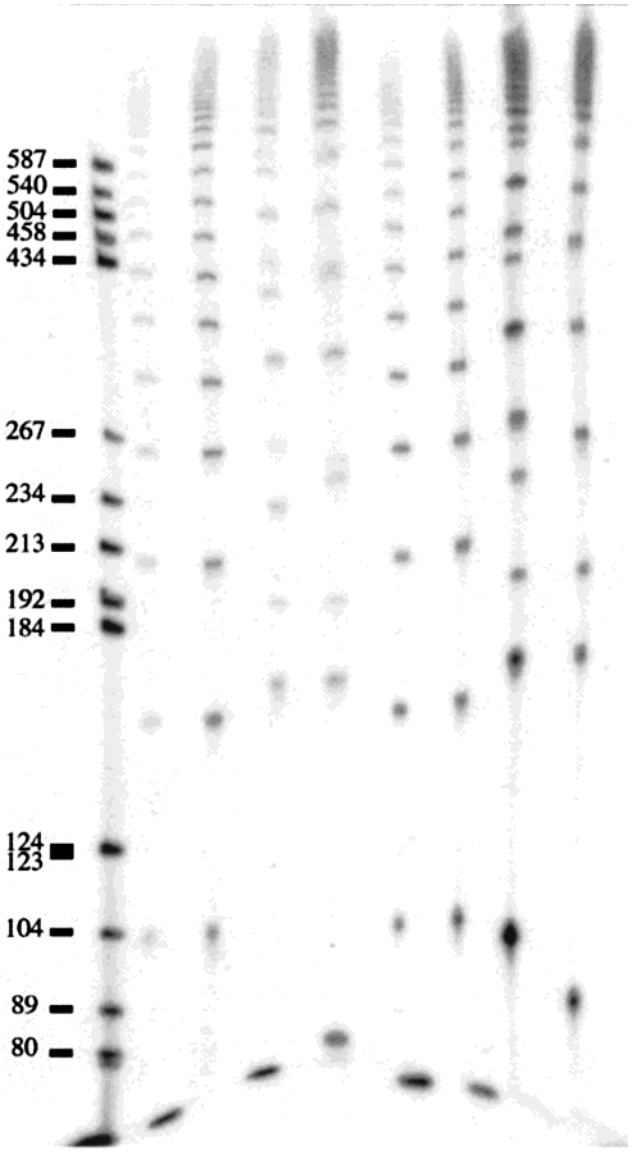

Figure 9. The ligation of molecules in a simple TX array. This is a denaturing autoradiogram displaying the products of ligating the **AB*** array shown in Figure 7. The leftmost lane contains a Hae III digest of pBR322, whose lengths are indicated. Proceeding rightward, there are eight pairs of lanes, the left of which contains one of the ligated strands, and the right of which contains the products of treating this material with exonucleases I and III. In order, these lanes contain strands A1, A2, A3, A4, B1, B2, B3, and B4. In no case is any cyclic material detectable in the exonuclease-treated lanes. This extent of sensitivity without harm to cyclic material is not uncommon in related systems (e.g., ref 32). Note that strand A1 is ligated to B1, and strand A2 is ligated to B2, where the A and B strands are the same length; hence, they produce uniform ladders on the gel; strand A3 is ligated to B4, and A4 is ligated to B3; strands 3 and 4 are not the same length, so an irregular ladder is visible for odd-length molecules, depending on whether an excess strand 3 or strand 4 is present in the ligated molecule.

(43) Balasubramanian B.; Pogozelski W. K.; Tullius, T. D. *Proc. Natl. Acad. Sci. U.S.A.* **1998**, *95*, 9738−9743.

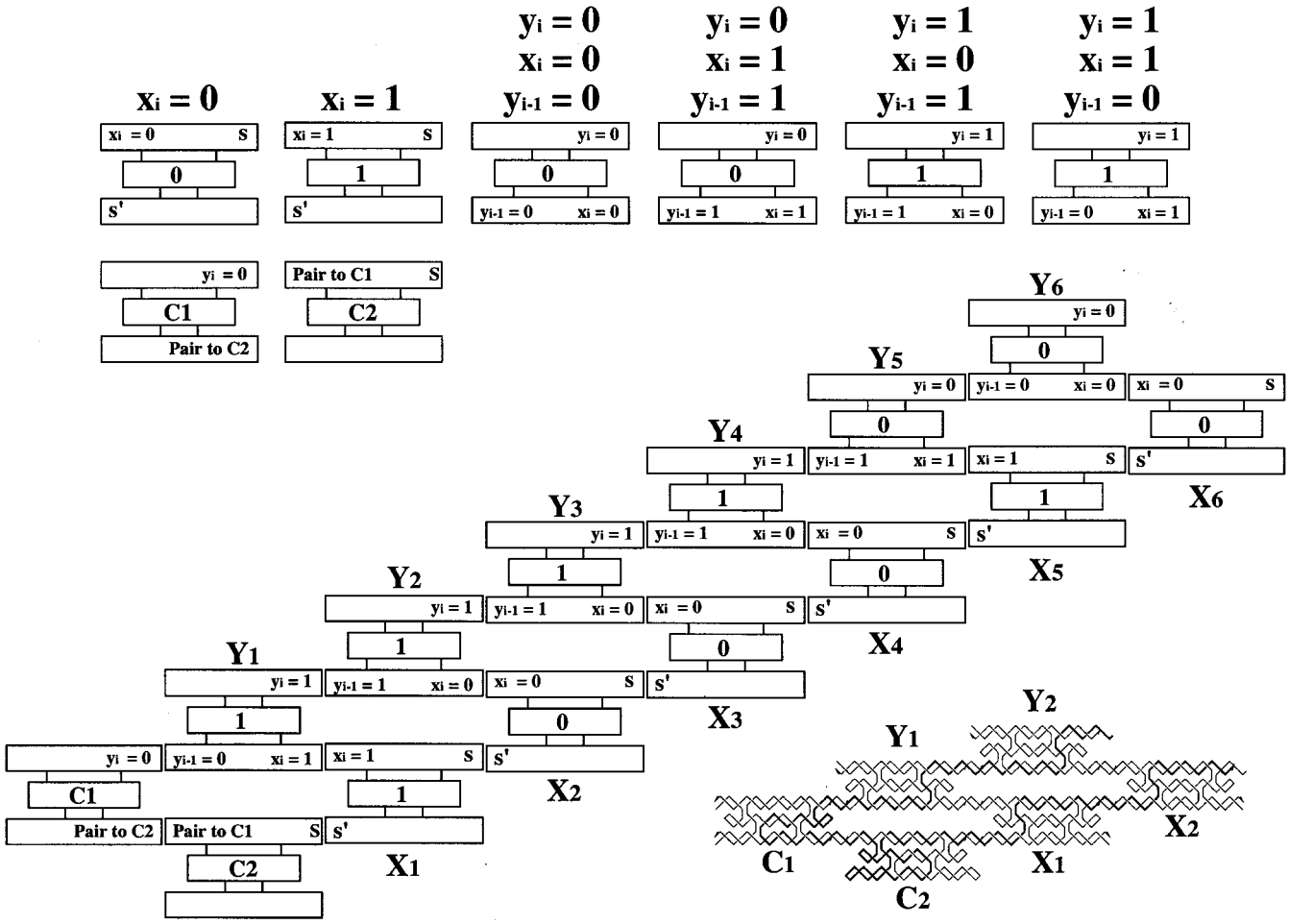

Figure 10. A cumulative XOR calculation performed with TX tiles. The eight component TX tiles for this calculation are shown at the top of the figure. The six tiles in the top row are needed to do the calculation. The two below them are needed to initiate the calculation properly. The value of each calculation tile is indicated by a "0" or "1" in the middle of its helical domain. The sticky ends (drawn flush) on the top and bottom helical domains are coded to have particular meanings. These meanings are indicated next to those termini. Note that all of these sticky ends are meant to be asymmetric, so that when the same meanings are shown to abut (e.g., $X_i = 0$ pairing with $X_i = 0$) this implies that the sequences are complementary, but not self-complementary. The expectation is that the tiles will assemble to form the proper arrangement, as shown in the array of tiles extending from the lower left to the upper right. The summation is designed to proceed from lower left to upper right. For example, at the end of the first cycle, $X_1 = 1$ and $Y_1 = 1$, because $Y_1 = X_1$. Note that the sticky end that binds C1 to Y_1 (labeled $Y_i = 0$) is set arbitrarily to bind to the sticky end of the tile corresponding to $Y_i = 1$, $X_i = 1$, and $Y_{i-1} = 0$. Through random binding, $X_2 = 0$ adds to the array. Whereas $X_2 \neq Y_1$, Y_2 should be 1, and only that tile fits properly between Y_1 and X_2. At the end of the assembly, the reporter strand running through the *X* diagonal array, around the corner, and then back up the *Y* diagonal array is ligated together to associate the calculated output with the input. The tiles in the calculation are left separated for clarity, but they are designed to generate a ligated strand structure. The strand structure in the vicinity of the corner is shown in the lower right portion of the figure. The thick strand is the reporter strand. Note that the Y_i tiles are upside down from the X_i tiles, a feature illustrated both in the strand drawing and in the tile assembly.

Discussion

TX Construction and Molecular Characterization. We find assembly of synthetic oligonucleotides into a well-behaved TX complex to be no more difficult than assembly of the simpler DX tiles described previously:[26] Analysis by nondenaturing gels indicates the formation of a complex with the expected stoichiometry; Ferguson analysis is in agreement with expectations; and the sites of the crossover points have been confirmed by hydroxyl radical autofootprinting. The lower portions of melting profiles of the TX and DX molecules examined track each other almost exactly when they enter their transition regions at about 55 °C. Thus, below this temperature the two molecules are likely to behave similarly and are likely to be of equal utility in DNA nanotechnology and DNA-based computation. As noted above, DX tiles have been examined in depth and shown to be sufficiently rigid that cyclization byproducts during ligation reactions are not a problem[32] and that ligation of tiles into much larger structures is successful.[10] TX tiles are likely to be similar to DX tiles in their rigidity, and we have shown that single-strand nicks between molecules are no more hidden from ligase than in DX tiles. Consequently, the prospects seem favorable to utilize TX tiles in larger covalent constructions.

Molecular Topology. The TX complex examined here consists exclusively of crossovers between helices separated by an odd number of double helical half-turns; one pair of helices is linked by crossovers separated by three half-turns, and the other pair is linked by crossovers separated by five half-turns. It is clear that it is possible to design triple crossover molecules whose helices are linked by crossovers separated by even numbers of half-turns or of mixtures of even and odd half-turns. The number of cyclic strands, analogous to those of DAE molecules, is a function of the separation of crossovers on each side of the central helical domain, as well as the separations of the crossovers on the same side of the helix. One useful feature of molecules with the topology explored here is that closing the ends in the two ways indicated in the corner tiles below in

Figure 10 permits reversal of reporter strand direction in an effective fashion (see below).

Self-Assembly and Ligation. We have assembled two different varieties of TX molecules to form two different two-dimensional arrays. One type, the TX and the TX+2J molecular combination (Figure 7), is very similar to the two-dimensional array reported recently for DX molecules.[10] The fact that we can perform this self-assembly suggests that the TX molecules are similar for assembly purposes to the DX molecules examined earlier, and that they are appropriate species to use in periodic two-dimensional applications. In contrast to the DX molecules, each molecule is flanked by a two nanometer gap, which could be used as a binding or tethering site for biological or molecular electronic components of the lattice. The array is as suitable for DNA-based computation as arrays built from DX units. The demonstration that it is possible to ligate the reporter strands extensively suggests that these TX arrays can be used for computational purposes, such as those described below and elsewhere.[44] It is clear that at least in the two-dimensional context linear reporter strands can be ligated up to lengths of roughly 15−20 units.

In addition to the assemblies analogous to those performed with DX molecules, we have also prepared a new type of assembly, in which the topographic marker is expected to be a rigid component of the system. This marker consists of another TX molecule but rotated by three nucleotides of the double helical repeat (ca. 103°) and sandwiched into one of the cavities of the TX array. We have found that orientations of the bulged junctions of the DX+2J motif are not rigid, and these additions are capable of flopping from side to side, even when coupled in pairs (Xu, G.; Mao, C.; Seeman, N. C., unpublished). By contrast, the rotated TX molecules are likely to display minimal flexibility in the directions about their central axes. This expectation is based on the torsional rigidity of the double helix, and it is currently under investigation.

Sample Computation. The means by which we expect TX molecules to be used in molecular computation requires explanation. Figure 10 illustrates a sample computation, a cumulative Exclusive OR (XOR) operation on a string of 1's and 0's. The result of the XOR operation is a 0 if two successive numbers are the same (0 and 0, or 1 and 1), but it is 1 if one of the two numbers is 0 and the other is 1. The cumulative XOR consists of a series of Boolean inputs $x_1,x_2,x_3 \ldots x_n$, and the output is also a series of Booleans, $y_1,y_2,y_3 \ldots y_n$, where $y_1 = x_1$, and for $i > 1$, $y_i = y_{i-1}$ XOR x_i. To do a specific cumulative XOR operation would require specific tags on tiles for each bit position on the sticky ends **S** and **S′** in Figure 10. However, the strength of molecular computation is that it can do every calculation in parallel using random self-assembly. Thus, the ends of the input tiles that direct their associations are deliberately encoded with the same sticky ends (**S** and **S′**), thereby producing many results in parallel.

Figure 10 shows that this computation requires two kinds of input tiles, corresponding to $x_i = 0$ and $x_i = 1$, and four kinds of output tiles, corresponding to [1] $y_i = 0$ because $x_i = 0$ and $y_{i-1} = 0$, [2] $y_i = 0$ because $x_i = 1$ and $y_{i-1} = 1$, [3] $y_i = 1$ because $x_i = 0$ and $y_{i-1} = 1$ and [4] $y_i = 1$ because $x_i = 1$ and $y_{i-1} = 0$. In addition, there are two initiator tiles required, the two corner tiles, C1 and C2. The reporter strand extends diagonally from the upper right of the x_nth tile, down through the corner tiles, where it reverses direction and proceeds diagonally back up through the output tiles. The 5′ end of the reporter strand produced in this fashion contains the cumulative XOR corresponding to the input sequence $x_1x_2...x_n$ on its 3′ end. Note, however, that the 5′→3′ order of the strand corresponds to $y_n...y_3y_2y_1...x_1x_2x_3...x_n$. Further details of this type of calculation and more complex computations are to be found in ref 44. The successful ligation of the periodic set of molecules described here bodes well for the correct ligation of a set of tiles capable of computation.

As a practical matter, it may be useful to use the techniques of solid-support-based DNA nanotechnology[7,45] to perform the calculation in a phased fashion. Thus, the corner tiles could be attached to a solid support, and X and Y tiles containing hairpins that occlude their sticky ends could be added one at a time and the reporter strands ligated. The sticky ends could then be liberated by restriction, or augmented restriction[46] (which produces longer sticky ends), before the next cycle proceeds. The advantage of this approach is that well-defined lengths of X and Y tiles would be attached to the growing array, and ligation failures could be destroyed.

Acknowledgment. We thank Dr. Brad Chaires for useful advice about DNA melting experiments. This work has been supported by grants NSF-CCR-97-25021 and CCR-96-33567 from DARPA and the National Science Foundation to J.H.R. and N.C.S., IRI-9619647 from NSF to J.H.R., ARO contract DAAH-0496-1-0448 to J.H.R., N00014-89-J-3078 from the Office of Naval Research to N.C.S., GM-29554 from the National Institute of General Medical Sciences to N.C.S., and F30602-98-C-0148 from the Air Force Research Laboratory Located at Rome, NY, to N.C.S.

JA993393E

(44) LaBean, T. H.; Winfree, E.; Reif, J. H. *Fifth Annual DIMACS Workshop on DNA Based Computers*; MIT: Cambridge, 1999.

(45) Zhang, Y.; Seeman, N. C. *J. Am. Chem. Soc.* **1992**, *114*, 2656−2663.

(46) Liu, F.; Wang, H.; Seeman, N. C. *Nanobiology* **1999**, *4*, 257−262.